

PHOTON STRUCTURE^a

STEFAN SÖLDNER-REMBOLD
CERN, CH-1211 Geneva 23, Switzerland
E-mail: stefan.soldner-rembold@cern.ch

The structure of the photon is probed in photon-photon interactions at LEP and in photon-proton interactions at HERA.

1 Photon structure ?

The photon is one of the fundamental gauge bosons of the Standard Model without self-couplings and without intrinsic structure. It couples to any kind of charged particle, which allows it to fluctuate directly into fermion-antifermion pairs and into bound states, vector mesons, which have the same spin-parity ($J^{PC} = 1^{--}$) as the photon. Photon-photon interactions therefore become possible through these quantum fluctuations.

At low energies photon-photon interactions can be studied e.g. in Delbrück scattering (elastic scattering of photons in the electric field of atoms) or in the elastic scattering process $\gamma\gamma \rightarrow \gamma\gamma$ where existing experimental limits using lasers are still 18 orders of magnitude above QED predictions¹. The knowledge of hadronic vacuum polarisations also still give the largest systematic error in the QED predictions for $g-2$ and for the running of the QED coupling constant².

The electron and positron beams at LEP and HERA can also be viewed as a copious source of high energy quasi-real and virtual photons. Interactions of photons are the hadronic processes with the largest cross-section at these experiments. At these high energies fluctuation times are longer than typical hadronic interaction time allowing the photon to develop a ‘structure’. The interactions of high energy photons can be described using structure functions and parton distributions of the photon in analogy to the interactions of real hadrons like the proton.

Why is it interesting to study photon structure ? Of course, it is simply important to understand the high energy scattering of a fundamental particle like the photon. Photon interactions are also sensitive to the quantum structure of the theory and can therefore be used to study QED and QCD. We can ask questions like: How similar to the proton is the photon ? How are the quarks and gluons distributed in the photon ? What happens if the photon becomes virtual ? At future linear colliders it will be very important to understand the

^ainvited talk given at DIS2000, Liverpool, UK, 25-30 April 2000

large number of events from photon interactions, and last but not least photon interactions can be an important probe to look for new physics, for example in the production of Higgs bosons at a photon linear collider ($\gamma\gamma \rightarrow H$)³.

2 Scales

“The photon and the proton, who is probing whom ?” asks Aharon Levy⁴. The same question can be asked for the interactions of two photons. The answer is related to the physical scales in the process. The situation looks simple if only one physical scale is large.

At LEP we denote the virtuality of the “probing” photon with $Q^2 = -q^2$ (the negative squared four-momentum of the photon) and the virtuality of the “probed” photon with $P^2 = -p^2 \approx 0$. Just like for the proton, the deep-inelastic scattering cross-section is then written as

$$\frac{d^2\sigma_{e\gamma \rightarrow e+\text{hadrons}}}{dx dQ^2} = \frac{2\pi\alpha^2}{xQ^4} [(1 + (1 - y)^2) F_2^\gamma(x, Q^2) - y^2 F_L^\gamma(x, Q^2)], \quad (1)$$

where α is the fine structure constant, x and y are the usual dimensionless variables of deep-inelastic scattering and $W^2 = (q + p)^2$ is the squared invariant mass of the hadronic final state. The scaling variable x is given by

$$x = \frac{Q^2}{Q^2 + W^2 + P^2}. \quad (2)$$

The term proportional to $F_L^\gamma(x, Q^2)$ is small and is therefore usually neglected. The structure function $F_2^\gamma(x, Q^2)$ can be identified with the sum over the parton densities of the photon weighted by the square of the parton’s charge. As a consequence deep-inelastic scattering mainly probes the quark structure of the photon, gluons only enter through scaling violations.

Another process in which photon structure can be studied is the production of (di-)jets in photon-proton (HERA) or photon-photon (LEP) interactions. The interacting photons are now almost real and the largest physical scale is the transverse energy of

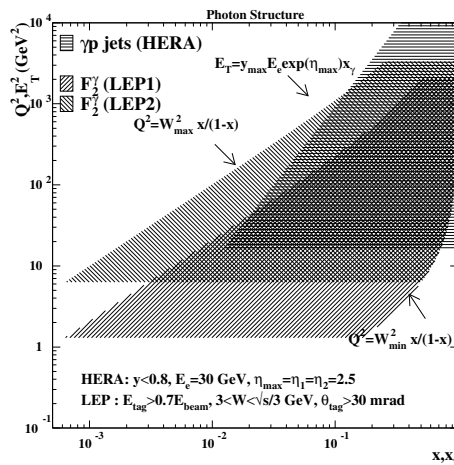


Figure 1: A comparison of the (Q^2, x) planes covered by LEP with the (E_T^2, x_γ) plane covered by HERA studying jet production.

the jets. The variable x_γ which is related to the fraction of the photon's momentum participating in the hard interactions can be reconstructed from the pseudorapidities η^{jet} and transverse energies E_T^{jet} of the jets:

$$x_\gamma = \frac{E_T^{\text{jet1}} e^{-\eta^{\text{jet1}}} + E_T^{\text{jet2}} e^{-\eta^{\text{jet2}}}}{2yE_e}, \quad (3)$$

where yE_e is the energy taken by the photon. In leading order, x_γ is equivalent to x and we can relate the parton distributions probed at LEP and HERA by $q_{\text{LEP}}(Q^2, x) \approx q_{\text{HERA}}((E_T^{\text{jet}})^2, x_\gamma)$. In jet production gluon induced processes dominate the cross-section in most kinematic regions, i.e. different from deep-inelastic electron-photon scattering the results are directly sensitive to the gluon distribution in the photon.

In Fig. 1 the kinematic range accessible at LEP and HERA is compared. At HERA accessing the low x parton densities of the photon requires the reconstruction of jets at low E_T^{jet} and large η^{jet} . This is experimentally difficult. In addition, additional soft or hard interactions of the photon's and the proton's remnant can take place which need to be disentangled from the primary hard scattering process.

3 How proton-like is the photon ?

The question should really be “How ρ -like is the photon ?”, but since we know much more about proton structure⁵ than ρ structure and since we study photon-proton interactions, we take the proton as a generic hadron for comparisons.

In a simple picture we can split the structure function F_2^γ into two parts, a Vector Mesons Dominance (VMD) part where the photon has fluctuated into a bound “hadron-like” state and a “point-like” part where the photon couples directly to a quark-antiquark pair. The original interest in the photon structure function was driven by the point-like part which can be calculated in the Quark-Parton-Model (QPM),

$$F_2^{\gamma, \text{QPM}}(x, Q^2) = \frac{N_c \alpha}{\pi} \sum_q e_q^4 x \left[(x^2 + (1-x)^2) \left(\ln \frac{Q^2}{m_q^2} - \ln \frac{x}{1-x} \right) - 1 + 8x(1-x) \right] \quad (4)$$

which is equivalent to the QED structure function. The structure function $F_2^{\gamma, \text{QPM}}(x, Q^2)$ rises linearly with $\ln \frac{Q^2}{m_q^2}$. It was first shown by Witten⁶ that this linear rise is still expected if QCD is turned on, however the parton mass m_q

is replaced by the QCD scale Λ_{QCD} . For asymptotically large Q^2 the structure function is fully calculable, including the normalisation. This is called the asymptotic prediction.

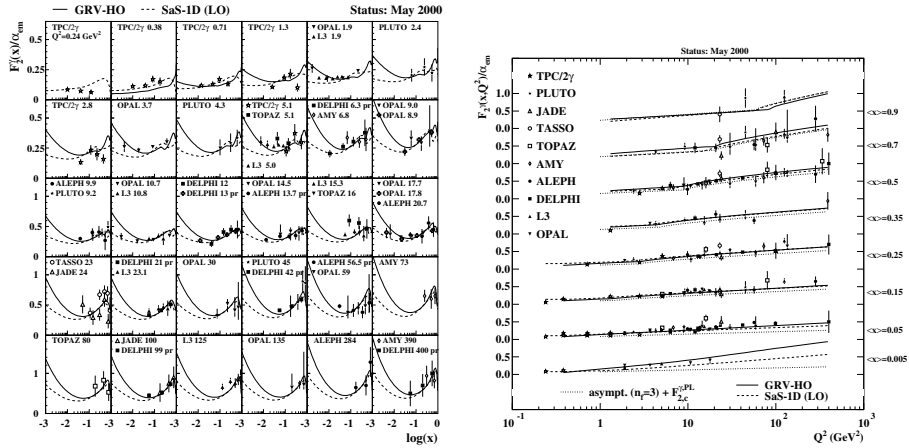


Figure 2: Measurements of the photon structure function F_2^γ in bins of x and Q^2 .

In the real world - far away from asymptotia - we have to take into account the non-perturbative “VMD-like” part for which some ansatz at small Q^2 is chosen and subsequently evolved with the inhomogeneous DGLAP equations. “Inhomogeneous” refers to the additional term which enters the evolution already in leading order, the perturbative splitting $\gamma \rightarrow q\bar{q}$. As a consequence the photon structure function exhibits positive scaling violations (it rises with Q^2) at all values of x , not only at low x as for the proton. This is the most striking difference between the photon and the proton.

4 How many gluons in a photon ?

At low x , approximately in the range $x < 0.1$, we expect that the structure function of the photon rises towards low x and with increasing Q^2 driven by the same QCD evolution as the proton structure function. Ideal processes to study the gluon in the photon are the production of (di-)jets and the production of heavy quarks in photon induced interactions.

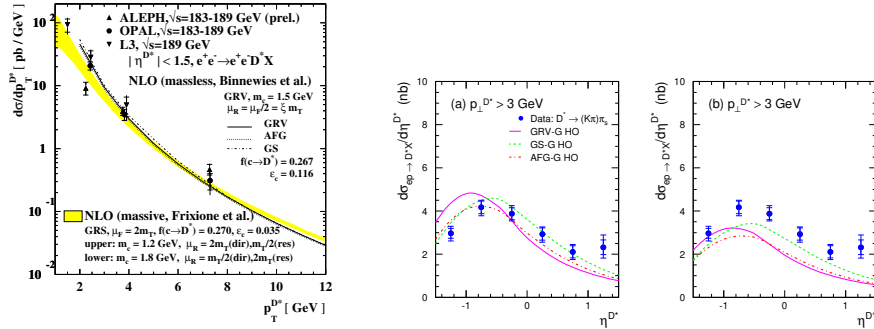


Figure 3: a) Differential cross-section $d\sigma/dp_T^{D^*}$ measured in photon-photon interactions by L3 and OPAL. b) Differential cross-section $d\sigma/d\eta^{D^*}$ measured by ZEUS in photoproduction compared to NLO calculations by Kniehl et al. ¹¹ (left) and by Cacciari et al. ¹² (right).

4.1 Charm in or from the photon ?

With charm a new scale enters, the mass m_c of the charm quark. The main LO contributions to open charm production in photon-photon interactions at LEP are the direct and the single resolved process. The single resolved photon-photon process is analogous to the direct photon-proton process where the gluon is taken from the proton and not from one of the photons. In both cases we can probe the gluon content, either of the photon or of the proton. Double resolved processes are negligible for open charm production in photon-photon interactions, but they are important in photoproduction.

The NLO calculations of open charm production are either done in the so-called massive or in the so-called massless scheme. In the massive scheme the mass m_c of the charm quark sets the scale for the perturbative QCD calculation. The cross-section is factorized into the matrix elements for the production of heavy quarks and the parton densities for light quarks (uds) and gluons. This ‘massive’ approach is expected to be valid if the transverse momenta p_T of the charm quarks are of the same order as the charm mass, $p_T \approx m_c$. In the ‘massless’ scheme, charm is considered as one of the active flavours in the parton distributions like u,d,s. This scheme is expected to be valid for $p_T \gg m_c$.

Open charm is usually tagged by measuring the production of D^* mesons. In Fig. 3a, the differential cross-section $d\sigma/dp_T^{D^*}$ measured in photon-photon interactions by L3 and OPAL ⁸ is compared to the NLO calculation by Frixione et al. ⁹ using the massive approach and to the NLO calculation by Kniehl

et al.¹⁰ using the massless approach. The massless calculation is in better agreement with the data than the massive calculation. In Fig. 3b, the differential cross-section $d\sigma/d\eta^{D^*}$ measured by ZEUS in photoproduction is compared to two different massless calculations, by Kniehl et al.¹¹ and by Cacciari et al.¹². The NLO calculations tend to underestimate the cross-section in the forward direction. Whereas in photon-photon scattering the massless cross-section seems to be nearly independent of the parton densities used, there seems to be more sensitivity to the choice of parametrisation in photoproduction.

4.2 Jet production

Another way to introduce a new hard scale in the process is to study jet production at large transverse momenta^{13,14,15}. Different groups have followed different philosophies for extracting information about the parton (mainly gluon) content of the photon from jet cross-sections. In the first approach hadronic jet cross-sections are measured and compared to NLO calculations which use different parametrisations of the photon's parton densities as input. In the second approach LO parton densities are extracted from the measurements.

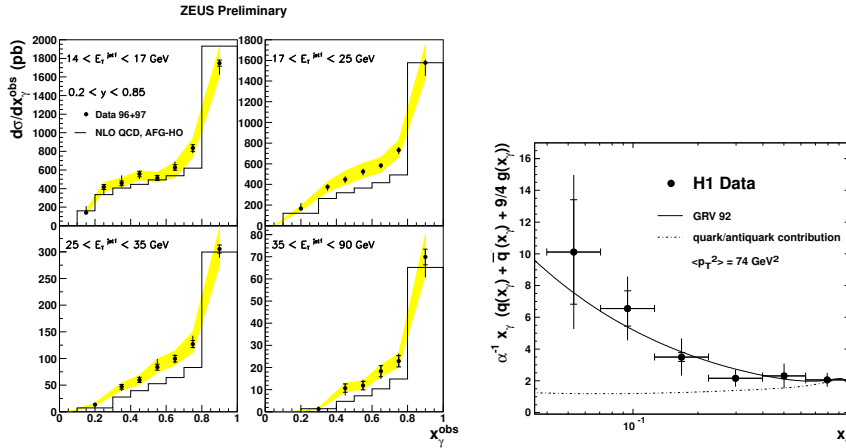


Figure 4: a) Differential cross-section $d\sigma/dx_\gamma^{\text{obs}}$ for different E_T^{jet} bins using jets in the range $-1 < \eta_{\text{jet}} < 2$ and $Q^2 < 1$ GeV² (ZEUS). b) Effective parton density of the photon for average jet transverse momenta $\langle p_T^2 \rangle = 74$ GeV² (H1).

In di-jet production the variable x_γ can be reconstructed from the momenta of the two jets. Fig. 4a shows a ZEUS measurement of the differ-

ential cross-section $d\sigma/dx_\gamma^{\text{obs}}$ for different E_T^{jet} bins using jets in the range $-1 < \eta_{\text{jet}} < 2$ and $Q^2 < 1 \text{ GeV}^2$ ¹⁴. The NLO calculations lie systematically too low which could indicate the need for more gluons in the parametrisations of the parton densities. NLO calculations are performed at the parton level and contain no hadronisation effects and also no underlying event. In addition, scale uncertainties have to be taken into account. For the high E_T^{jet} region considered here, these effects are expected to be small enough so that the discrepancy between data and the NLO calculations can be attributed to inadequacies of the parametrisations of the parton densities.

The second approach to extract effective parton densities is shown in Fig. 4b. The effective parton densities are extracted from the di-jet data assuming a similar angular distribution for all resolved processes¹⁵. The effective parton density of the photon is given by

$$\tilde{q}_\gamma(x_\gamma, p_T^2) \equiv \sum_{n_f} (q_\gamma(x_\gamma, p_T^2) + \bar{q}_\gamma(x_\gamma, p_T^2)) + \frac{9}{4}g_\gamma(x_\gamma, p_T^2). \quad (5)$$

The LO quark density $q_\gamma(x_\gamma, p_T^2) + \bar{q}_\gamma(x_\gamma, p_T^2)$ is reasonably well constrained by e^+e^- data in this kinematic range and its contribution - shown as dashed line in Fig. 4 - is small. If the quark distribution is subtracted, a clear rise of the gluon distribution towards low x can be observed.

5 Parton densities of the virtual photon

Until now we have studied the structure of (quasi-)real photons, i.e. $P^2 \approx 0$ (LEP) or $Q^2 \approx 0$ (HERA). In e^+e^- collisions the effective structure function of virtual photons can be measured if $Q^2 \gg P^2 \gg \Lambda_{\text{QCD}}$. This was first done by PLUTO¹⁶. For real photons only the cross-sections σ_{LT} and σ_{TT} contribute, where the indices refer to the longitudinal and transverse helicity states of the probe and target photon, respectively, i.e. $F_2^\gamma \simeq \sigma_{\text{LT}} + \sigma_{\text{TT}}$. For $P^2 \gg 0$ other helicity states have to

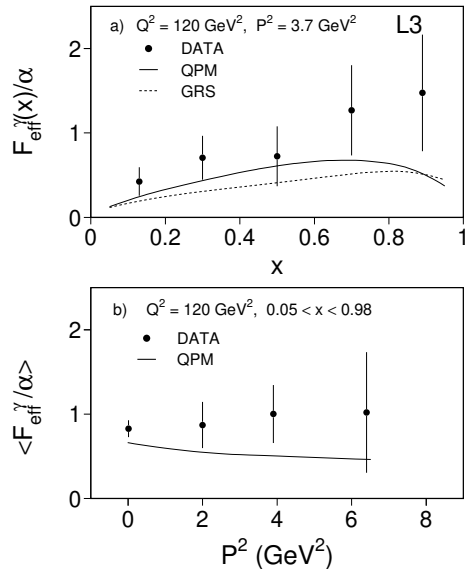


Figure 5: Effective structure function measured by L3 as function of x and P^2 .

be taken into account, leading to the definition of the effective structure function $F_{\text{eff}}^\gamma \simeq \sigma_{\text{LT}} + \sigma_{\text{TT}} + \sigma_{\text{TL}} + \sigma_{\text{LL}}$ (interference terms are neglected here). This effective structure function has been measured by L3 and is shown in Fig. 5. We expect the non-perturbative part of the parton densities (VMD) at low x to decrease with increasing virtuality of the photon. Compared to the data as a function of P^2 in Fig. 5b, the QPM prediction therefore fails to describe the point at $P^2 = 0$. The shape of the P^2 dependence is consistent with the simple QPM ansatz but the errors are still large. Much more precise data is to be expected from LEP on the structure of the virtual photons in the next years.

6 $\gamma^*\gamma^*$ scattering

For studying the effective structure function of virtual photons, we assumed that $Q^2 \gg P^2$. In the special case where both photons have large and approximately equal virtualities, $Q^2 \approx P^2$ (or better $Q_1^2 \approx Q_2^2$), the structure function formalism can no longer be applied.

For sufficiently large virtualities this process has been called the ‘optimal test’ of the prediction of the BFKL formalism¹⁷. The condition $Q_1^2 \approx Q_2^2$ ensures that DGLAP evolution is suppressed. The application of the BFKL formalism to $\gamma^*\gamma^*$ scattering has been considered by^{18,19,20}. A sketch of the main diagrams is shown in Fig. 6a.

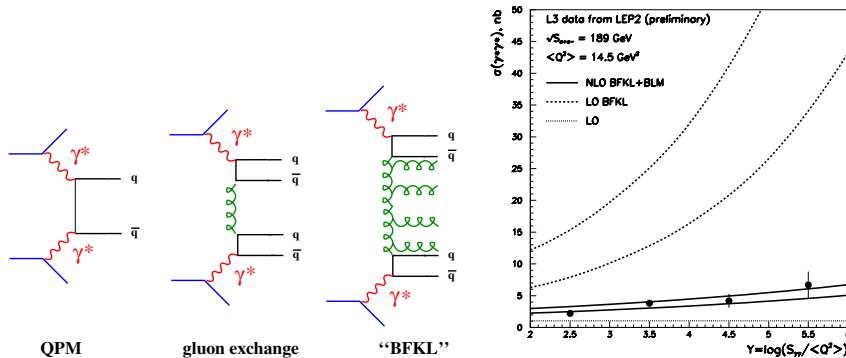


Figure 6: a) Different diagrams which are expected to contribute to $\gamma^*\gamma^*$ scattering: QPM (Quark Parton Model), single gluon exchange and the ‘BFKL’ process. b) the hadronic $\gamma^*\gamma^*$ cross-section measured by L3 as a function of Y compared to the calculations of¹⁹.

In the BFKL formalism there is a problem at LO in setting the two mass scales on which the cross-section depends: the mass at which the strong cou-

pling α_s is evaluated and the mass which provides the scale for the high energy logarithms. The result is very sensitive to these parameters²⁰. An additional uncertainty is due to the correct treatment of the production of massive charm quarks¹⁷.

From the LO BFKL prediction an approximately exponential increase of the hadronic cross-section $\sigma(\gamma^*\gamma^*)$ is expected as a function of the variable

$$Y \approx \ln \frac{W^2}{\sqrt{Q_1^2 Q_2^2}}. \quad (6)$$

The LO BFKL cross-section is significantly too high compared to the L3 data shown in Fig. 6b where the data are compared to the calculations of¹⁹. A prediction which includes an estimate of the NLO effects is also shown. The NLO curves are much closer to the data. It is also interesting to note that the LO Monte Carlo PHOJET is consistent with the data within the large experimental errors, apart from the very high Y region where deviations are seen. Both, the theoretical and experimental uncertainties are still large and require further study before more quantitative conclusions can be drawn²¹.

7 Conclusions

The amount of interesting data from LEP and HERA on the structure of real and virtual photons has increased so much in the last years that only a few highlights can be mentioned in such a brief write-up. I have not discussed the interesting H1 measurements of the effective parton densities of the virtual photons, the ZEUS measurements of the suppression of the resolved component with increased photon virtuality, the OPAL measurement of the charm structure function of the photon, and many other topics.

It becomes more and more clear that we need a common quantitative understanding of the LEP and HERA data on photon structure, especially in the form of new parton densities which make use of the new precise data from LEP and HERA. To accomplish this, we also still need a better understanding of the non-perturbative effects (hadronisation, underlying event) which still lead to systematic limitations in the interpretation of the data.

Acknowledgments

I would like to thank John Dainton and his colleagues from Liverpool for organising this interesting and exciting conference.

References

1. D. Bernard, Nucl. Phys. B (Proc. Suppl.) 82 (2000) 439.
2. M. Davier, A. Höcker, Phys. Lett. B435 (1998) 427.
3. M. Melles, Nucl. Phys. B (Proc. Suppl.) 82 (2000) 379; G. Jikia, S. Söldner-Rembold, Nucl. Phys. B (Proc. Suppl.) 82 (2000) 373.
4. A. Levy, Proc. of 1999 KEK-Tanashi Symposium, hep-ph/0002015.
5. M. Erdmann, these proceedings.
6. E. Witten, Nucl. Phys. B120 (1977) 189.
7. ZEUS Collaboration, J. Breitweg et al., Eur. Phys. J. C6 (1999) 67.
8. L3 Collaboration, M. Acciarri et al., Phys. Lett. B467 (1999) 137; OPAL Collaboration, G. Abbiendi et al., hep-ex/9911030.
9. S. Frixione et al, hep-ph/9908483.
10. J. Binnewies, B.A. Kniehl and G. Kramer, Phys. Rev. D58 (1998) 014014; Phys. Rev. D53 (1996) 6110.
11. B. A. Kniehl et al., Z. Phys. C76 (1997) 689.
12. M. Cacciari et al., Phys. Rev. D55 (1997) 2736; *ibid* 7134.
13. E. Heaphy, B. Surrow, A. Valkarova, these proceedings.
14. M. Wing, these proceedings, hep-ex/0007011.
15. S. Maxfield, these proceedings; H1 Collaboration, C. Adloff et al., Phys. Lett. B483 (2000) 36.
16. PLUTO Collaboration, C. Berger et al., Phys. Lett. B142 (1984) 119.
17. J. Bartels, C. Ewerz, R. Staritzbichler, hep-ph/0004029.
18. F. Hautmann: Proceedings of the XXVIII International Conference on High Energy Physics ICHEP96 (Warsaw, July 1996), eds. Z. Ajduk and A.K. Wroblewski, World Scientific, p.705; J. Bartels, A. De Roeck and H. Lotter: Phys. Lett. B389 (1996) 742; M. Boonekamp, A. De Roeck, C. Royon and S. Wallon: hep-ph/9812523; J. Kwiecinski and L. Motyka: Phys. Lett. B462 (1999) 203; N.N. Nikolaev, J. Speth, V.R. Zoller, hep-ph/0001120;
19. V.T. Kim, L.N. Lipatov, G. Pivovarov hep-ph/9911242, hep-ph/9911228;
20. S.J. Brodsky, F. Hautmann and D.E.Soper: Phys.Rev.Lett. 78 (1997) 803; Erratum *ibid* 79 (1997) 3544; S.J. Brodsky, F. Hautmann and D.E. Soper: Phys.Rev. D56 (1997) 6957.
21. A. Donnachie, C.-H. Lin, L. Lipatov, E. Naftali, these proceedings.